FORMULATION OF POST-PEAK BEHAVIOR OF OLD REINFORCED CONCRETE COLUMNS UNTIL COLLPASE

Manabu Yoshimura [1]

[1] *Professor, Graduate School of Architecture and Building Engineering, Tokyo Metropolitan University, Japan*
Email: myoshim@arch.metro-u.ac.jp

ABSTRACT :

RC buildings designed by the Japanese codes older than 1971 are in danger of suffering heavy damages or even collapse during severe earthquakes. To evaluate seismic performance of those buildings more accurately than a present level, it is necessary to grasp post-peak behavior of old columns. Half-scale model specimens representing old columns that were designed to fail in shear or flexural yielding were tested until they came to be unable to sustain gravity load. Based on test results, the post-peak behavior of old columns until collapse was examined and formulated.

KEYWORDS: Reinforced concrete, Collapse, Shear failure, Flexural yielding, Post-peak behavior

1. INTRODUCTION

AS for ductile structures, various methods including pushover analysis and nonlinear time history analysis are available and their results are deemed reliable too. However, as for brittle structures such as those constructed before 1971, when the seismic requirements for shear became stringent in Japan, these analyses, even if applied, are not expected to produce reliable results, because the post-peak behavior of brittle columns is not well known. Therefore, the Standard for Seismic Evaluation of Existing RC Buildings (Evaluation Standard, 2001) is still the only way in Japan that can be used to evaluate the seismic performance of old structures.

Under such a situation, it was intended in this study to examine and formulate the post-peak behavior of old columns until gravity load collapse. Discussions are focused on the reason of collapse, lateral drift vs. lateral load relations and lateral drift vs. axial deformation relations.

2. COLLAPSE BEHAVIOR

2.1. Outline of Tests

Old columns, although fail in shear in most cases, occasionally fail in flexure when they are long. Thereby, half-scale model specimens with both failure types, twenty six in total number, were fabricated and tested (Yoshimura et al. 2005). Hereafter, shear-failing type is referred to as S-mode while flexural-yielding type as F-mode. However, note all specimens including the F-mode were classified as "Shear Column" in the Evaluation Standard, where classified so if computed shear strength was smaller than computed flexural strength. Test variables were, transverse-bar ratio (p_w, transverse-bar area divided by column width multiplied by transverse-bar spacing), axial-stress ratio (η, axial load divided by column area multiplied by concrete strength), longitudinal-bar ratio (p_g, total longitudinal-bar area divided by column area), and clear height ratio (h_0/D, column clear height divided by column depth).

Test apparatus is shown in Figure 1, where the pantograph was placed so that the loading beam at the column top might not rotate (double curvature deformation might be realized). A loading method was as follows. The specimens were loaded to the lateral direction under constant axial load. The vertical actuator was controlled by load while the lateral actuator was by displacement. And the test was terminated by the limiter of the vertical actuator that was set to operate just when collapse occurred and column axial shortening reached 50mm.

A ratio of computed shear strength to computed flexural strength, strength ratio, is conventionally used as an index to assess column deformability. The relations between that ratio and collapse drift (lateral drift at collapse) are shown in Figure 2. The border of the two modes lies near the strength ratio of 0.7, considerably smaller than unity. It is because of the safety factor incorporated in the computed shear strength. The amplitudes of collapse drift are found to range very widely for both modes.

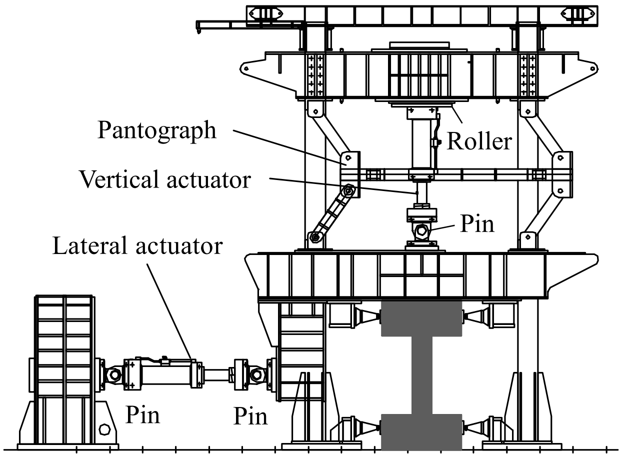

Figure 1 Test apparatus

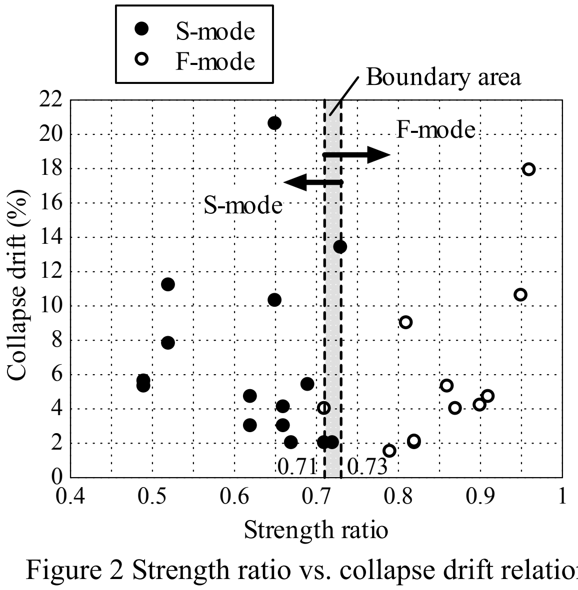

Figure 2 Strength ratio vs. collapse drift relations

2.2. Collapse of S-mode Specimens

The results of an S-mode specimen are shown in Figure 3. The occurrence of collapse was not soon later than shear failure, but was when the main shear crack widened and lateral load decreased to nearly zero. The collapse accompanied the buckling of longitudinal bars. All S-mode specimens exhibited similar collapse behavior. The reasons of bar buckling were, 1) the increase of axial compression carried by longitudinal bars resulting from the widening of the main shear crack, and 2) the decrease of compression capacity of these bars due to the local flexural deformation near the crack. In short, the reason of collapse for the S-mode specimens was the failure of longitudinal bars.

2.3. Collapse of F-mode Specimens

The results of an F-mode specimen are shown in Figure 4. The collapse that occurred very suddenly without showing clear strength reduction, accompanied severe concrete crushing at the column end. All F-mode specimens exhibited similar collapse behavior. The reason of collapse for F-mode specimens was the failure of concrete.

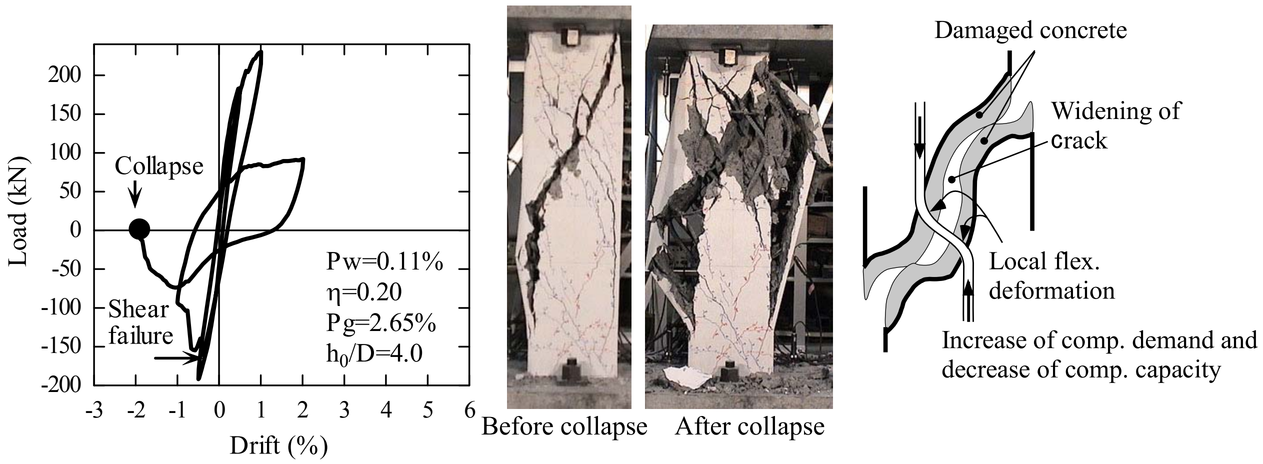

Figure 3 Collapse of S-mode specimen (Specimen No.3)

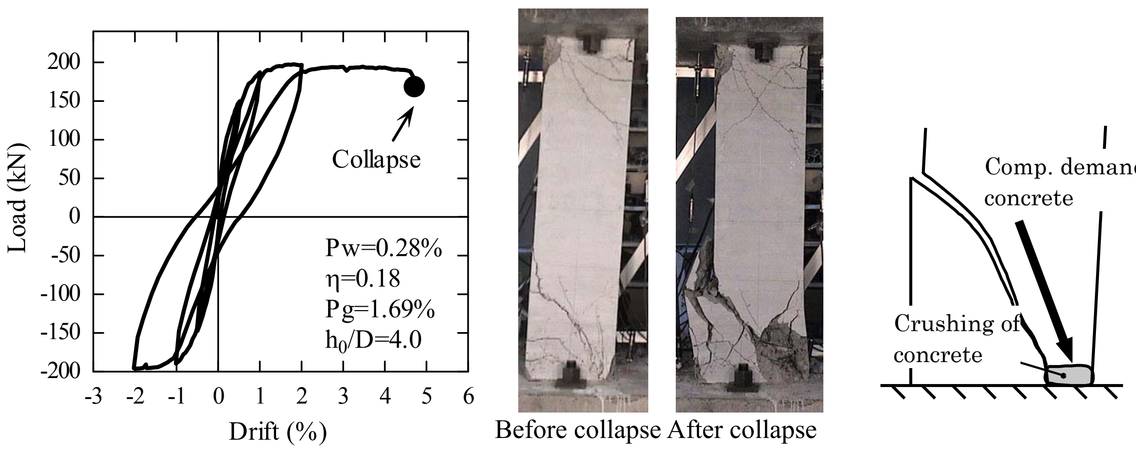

Figure 4 Collapse of F-mode specimen (Specimen Y28L)

3. EVALUATION OF COLLAPSE DRIFT AND DRIFT VS. LOAD RELATIONS

It was attempted to evaluate collapse drift based on the test results. The strength ratio is widely used to evaluate column deformability, for example, lateral drift associated with maximum load. However, Figure 2 does not show the trend that collapse drift becomes larger as the strength ratio is greater, indicating this ratio is not proper to evaluate collapse drift.

Thus, the effect of main test variables, transverse-bar ratio, axial-stress ratio and longitudinal-bar ratio on collapse drift was studied. As for transverse-bar ratio and axial-stress ratio, collapse drift became larger as the former was larger and as the latter was smaller. It held true for both modes. These results were natural.

However, as for the effect of longitudinal-bar ratio, collapse drift became larger for the S-mode as it was larger while did larger for the F-mode as it was smaller (Figure 5). In other words, the effect of longitudinal-bar ratio was opposite for both modes. It is apparent that such results are related to the reason of collapse stated earlier. For the S-mode the large amount of longitudinal bars is advantageous because collapse is controlled by longitudinal bars while for the F-mode the small amount of them is advantageous because collapse is controlled by concrete. See Figure 2 again. One can read the trend for the S-mode that collapse drift became larger except for two plots with drift more than 12% (only both cases showed bond-splitting failure after shear failure) as the strength ratio was smaller, or flexural strength was larger, or amount of longitudinal bars was larger, and the opposite trend for the F-mode.

Moehle et al. who proposed equations to predict collapse drift using the shear-friction model, reported good agreements of the predicted and observed values (Moehle et al. 2002). Note their specimens were mostly of the F-mode according to our definition. However, if it is considered there are two types of collapse depending on the failure mode, it seems difficult to express collapse by a single model. Then, it was attempted to form an empirical equation for each mode. It was assumed collapse drift was expressed as a linear combination of the three main variables, and each coefficient was determined by the least square method. The best fitted equations giving collapse drift (R_u) are as follows, where R_u, p_w and p_g are in %.

For the S-mode, $$R_u = 62.2 \cdot p_w - 51.9 \cdot \eta + 6.07 \cdot p_g - 9.91 \geq 1.5 \qquad (3.1)$$

And for the F-mode, $$R_u = 28.0 \cdot p_w - 42.3 \cdot \eta - 8.60 \cdot p_g + 20.6 \geq 1.5 \qquad (3.2)$$

Note the coefficients on longitudinal-bar ratio are positive and negative, respectively for the S-mode and F-mode (the reason of this was stated earlier). The observed and evaluated values are compared in Figure 6.

The skeleton curves of drift vs. load relations, idealized as quadrilinear system, were proposed based on the evaluated collapse drift. Examples of evaluated skeleton curves are shown in Figure 7. It was assumed that strength reduction was large for the S-mode (zero load at collapse) while small for the F-mode. Detailed descriptions for the evaluated skeleton curves are found in another paper (Yoshimura et al. 2005).

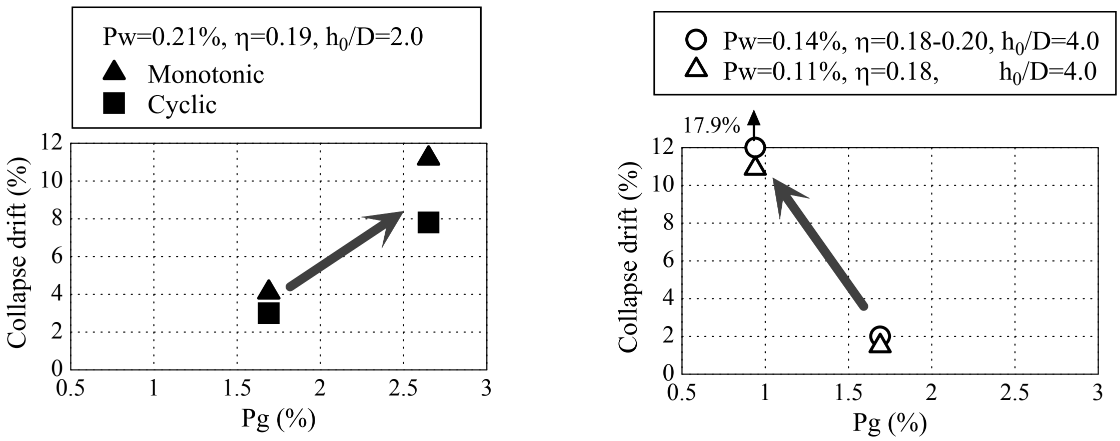

(a) S-mode (b) F-mode

Figure 5 Longitudinal-bar ratio vs. collapse drift relations

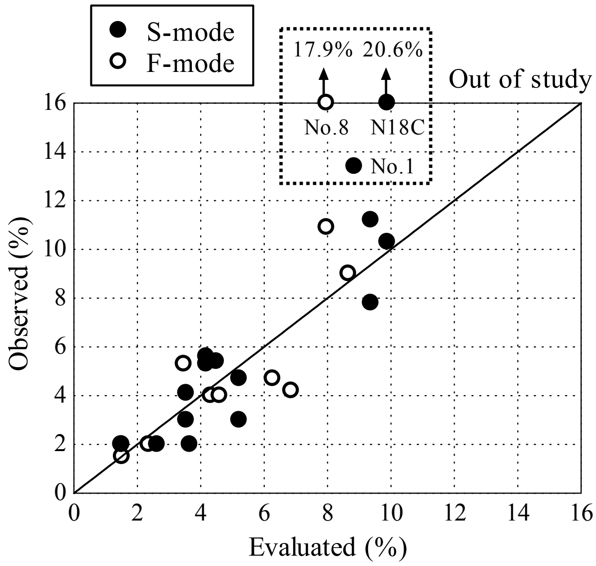

Figure 6 Comparison of collapse drift

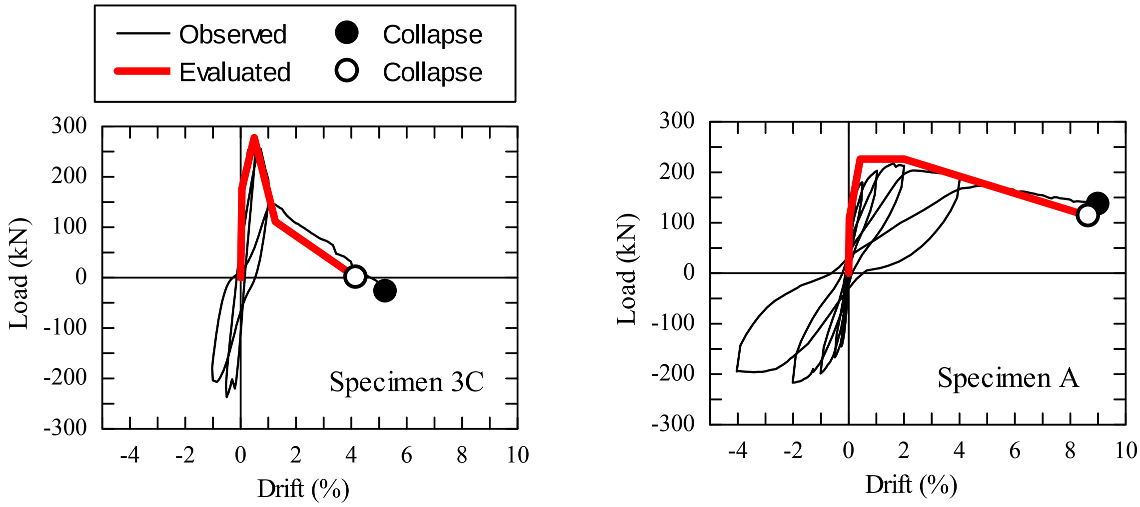

(a) S-mode (b) F-mode

Figure 7 Lateral drift vs. lateral load relations

4. EVALUATION OF AXIAL DEFORMATION FOR S-MODE

Lateral drift vs. axial deformation relations for an S-mode specimen are shown in Figure 8. And the slope of these relations, defined as a ratio of axial deformation increment to lateral drift increment at each step, is shown in Figure 9. In both figures, “Approximated” denotes the case where lateral drift vs. axial deformation relations were smoothed by using a cubic equation. The Slope after shear failure is found to increase with the increase of lateral drift, or the decrease of lateral load.

The reason why the Slope increases as the loading proceeds is discussed below (Nakamura et al. 2002). Figure 10(b) shows a conceptual sketch of lateral-load and axial-load interaction curve (failure surface). The initial failure surface that corresponds to the state of maximum load, is assumed as represented by a quadratic equation. Note the points of initial axial compression strength and initial axial tension strength lie on it. It is believed that the failure progress that occurs after maximum load accompanies the deterioration of concrete, resulting in the reduction of axial compression strength as well as lateral (shear) strength. But axial tension strength is considered to keep an initial value because it is not affected by the deterioration of concrete. The contracted failure surface in the figure is determined by considering the above and assuming its shape is similar to that of the initial failure surface. By the way, one knows from the flow rule in plastic theory that the direction of incremental plastic deformation, n is normal to the failure surface. And the Slope defined earlier coincides with this direction. Though exactly speaking the Slope has to be based on plastic deformation (actually based on total deformation), it is not a problem because elastic deformation is very small. As is shown in the figure, n, therefore, the Slope increases as the loading proceeds (failure surface is contracted), which agrees with the observations (Figure 9).

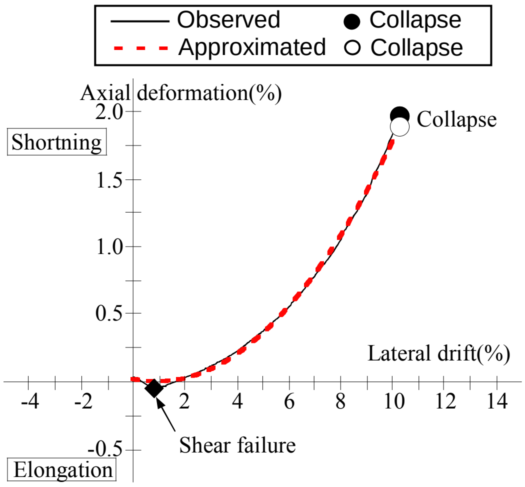

Figure 8 Lateral drift vs. axial deformation relations (Specimen N18M)

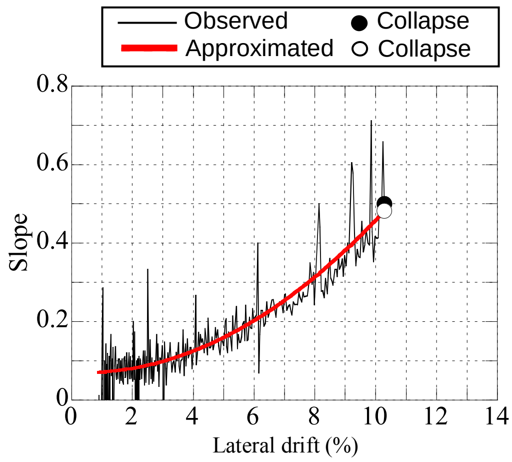

Figure 9 Lateral drift vs. slope relations (Specimen N18M)

Based on the above discussions, lateral drift vs. axial deformation relations were formulated (Figure 10). The procedures are as follows. Firstly lateral drift, R vs. lateral load, P relations are determined from the idealized skeleton curve (Figure 7). Accordingly, P is expressed as a function of R. Secondly the Slope, n is expressed by a function of P, resulting that the Slope, n is expressed by a function of R. Then by integrating n with respect to R, one can get lateral drift vs. axial deformation relations. An example of the evaluation is shown in Figure 11. The agreement with the observations is fairly good.

The method proposed above has the following practical use. It is thought that for columns that fail in shear during earthquakes, residual axial deformation that can be measured after earthquakes does not differ much from the axial deformation associated with maximum lateral drift attained during earthquakes. If it is assumed, the maximum lateral drift and reduction of lateral load associated with it are predicted from the measured residual axial deformation. This idea was applied to a specimen (Figure 12). In the figure, the residual axial deformation is considered as axial deformation at the zero lateral drift after +4% lateral drift. It proves that the assumption stated above is proper and that the point (white diamond shape) predicted as maximum lateral drift is close to the observations (black diamond shape).

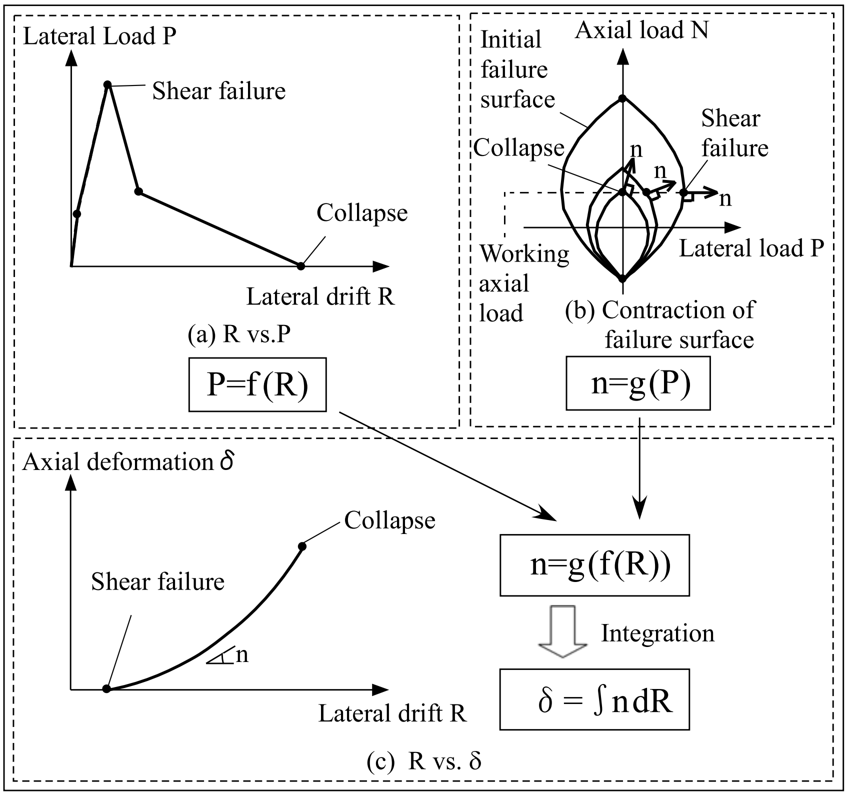

Figure 10 Evaluation of axial deformation

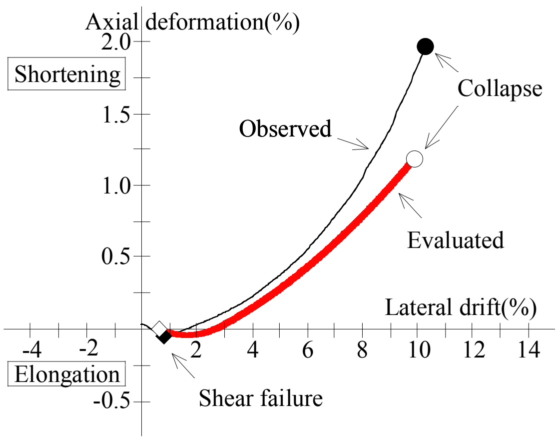

Figure 11 Comparison of lateral drift vs. axial deformation relations (Specimen N18M)

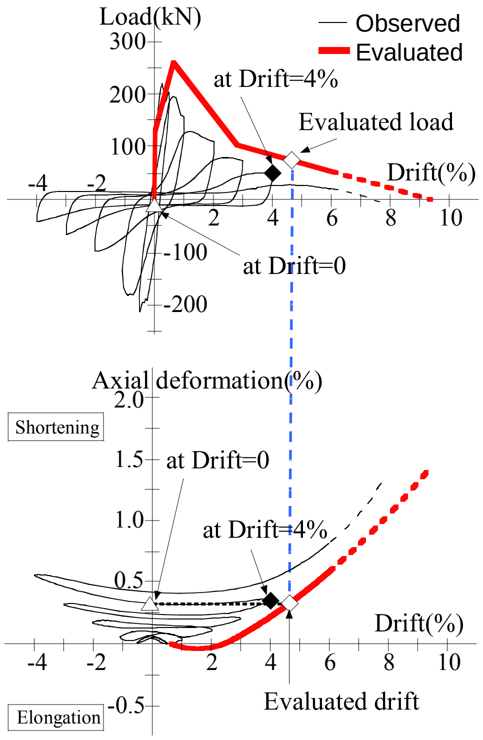

Figure 12 Evaluation of maximum drift, and load reduction (Specimen 2C)

5. COCLUSIONS

It was attempted to examine and formulate the post-peak behavior of old columns until collapse. The major findings from the study are as follows.

1) For the S-mode, collapse occurs when lateral load decreases to nearly zero. The reason of collapse is the failure of longitudinal bars, resulting collapse drift becomes larger with the increase of longitudinal-bar ratio.
2) For the M-mode, collapse occurs very suddenly without clear strength reduction. The reason of collapse is the failure of concrete, resulting collapse drift becomes larger with the decrease of longitudinal-bar ratio.
3) The equations giving the skeleton curves of drift vs. load relations until collapse were proposed for each mode.
4) The method to evaluate axial deformation for the S-mode was proposed, where the contraction of failure surface and flow rule were used.

ACKNOWLEDGEMENTS

The author expresses his special gratitude to Drs. Takaya Nakamura and Yoshikazu Takaine, who assisted him in studying in this text.

REFERENCES

Japan Association for Building Disaster Prevention (2001). Standard for Seismic Evaluation of Existing RC Buildings (in Japanese)

Yoshimura, M. and Takaine, Y. (2005). Formulation of post-peak behavior of reinforced concrete columns including collapse drift, Journal of Construction Engineering, Architectural Institute of Japan, **No.587**, 163-171. (in Japanese)

Moehle, J. P., Elwood, K. J., and Sezen, H. (2002). Gravity load collapse of building frames during earthquakes, ACI SP-197, Behavior and Design of Concrete Structures for Seismic Performance, American Concrete Institute, 215-238.

Nakamura, T. and Yoshimura, M. (2002). Gravity load collapse of reinforced concrete columns with brittle failure mode, Journal of Asian Architecture and Building Engineering, Architectural Institute of Japan, **vol.1 no.1**, 21-27.